CrossMark

ORIGINAL PAPER

Estimation of aboveground tree carbon stock using SPOT-HRG data (a case study: Darabkola forests)

Masoumeh Fatholahi[1] · Asghar Fallah[1] · Seyed Mohammad Hojjati[1] · Siavash Kalbi[1]

Abstract Forests are among the most important carbon sinks on earth. However, their complex structure and vast areas preclude accurate estimation of forest carbon stocks. Data sets from forest monitoring using advanced satellite imagery are now used in international policy agreements. Data sets enable tracking of emissions of CO_2 into the atmosphere caused by deforestation and other types of land-use changes. The aim of this study is to determine the capability of SPOT-HRG Satellite data to estimate aboveground carbon stock in a district of Darabkola research and training forest, Iran. Preprocessing to eliminate or reduce geometric error and atmospheric error were performed on the images. Using cluster sampling, 165 sample plots were taken. Of 165 plots, 81 were in natural habitats, and 84 were in forest plantations. Following the collection of ground data, biomass and carbon stocks were quantified for the sample plots on a per hectare basis. Nonparametric regression models such as support vector regression were used for modeling purposes with different kernels including linear, sigmoid, polynomial, and radial basis function. The results showed that a third-degree polynomial was the best model for the entire studied areas having an root mean square error, bias and accuracy, respectively, of 38.41, 5.31, and 62.2; 42.77, 16.58, and 57.3% for the best polynomial for natural forest; and 44.71, 2.31, and 64.3% for afforestation. Overall, these results indicate that SPOT-HRG satellite data and support vector machines are useful for estimating aboveground carbon stock.

Keywords Aboveground carbon stock · Support vector machine · SPOT-HRG · Darabkola

✉ Masoumeh Fatholahi
  Massomefatholahi@ymail.com

  Asghar Fallah
  Fallaha2007@yahoo.com

  Seyed Mohammad Hojjati
  S_M_hodjati@yahoo.com

  Siavash Kalbi
  S.kalbi63@gmail.com

[1] Department of Natural Resource, Sari University of Agricultural Sciences and Natural Resources, Sari, Mazandaran 48151, Iran

Introduction

The global carbon cycle is a major issue in global climate change research. As the largest terrestrial ecosystem, the forest ecosystem and carbon exchange within it have an important influence on the global carbon balance. Estimating aboveground forest biomass is thus the most important step in measuring carbon stocks and fluxes from forests and helps to determine the contribution of forests to the global carbon cycle (Vicharnakorn et al. 2014). An estimate of forest biomass also provides an important reference point for global carbon and carbon cycle research (Dong et al. 2013; IPCC 2000).

The amount of carbon sequestered by a forest can be inferred from its biomass accumulation because approximately 50% of forest dry biomass is carbon (Brown 1997a, b; Vicharnakorn et al. 2014). The bulk of biomass assessments are performed on aboveground biomass

(AGB) of trees since it generally represents the greatest fraction of the total living biomass in a forest and does not pose significant logistical problems during field measurements (IPCC 2007; Vicharnakorn et al. 2014). Forest inventories can be used to determine the spatiotemporal distribution of aboveground forest carbon pools, but they require substantial amounts of time and money and are limited to five years (Goetz et al. 2009).

Satellite data make it possible to monitor and map forests and to trace changes in forest biomass and carbon stock (Eckert 2012). A great deal of research has been devoted to remote sensing-based estimations of biomass, as interdependencies between remote sensing data and biomass have been increasingly discovered for empirical methods when compared to more complicated approaches based on physical mechanism models (Liu et al. 2015).

A common approach is to apply regression analyses to the reflectance channels and spectral and textural indices based on information from sampling sites (Steininger 2000; Castillo-Santiago et al. 2010). Recently, nonparametric algorithms have been explored to estimate forest attributes because of advantages such as flexibility and ability to describe nonlinear dependencies compared with parametric algorithms (Sironen et al. 2010). One particularly useful advantage of nonparametric algorithms is that they are free from assumptions of any given probability distribution and observations are assumed to be independent (Sironen et al. 2010). Machine-learning algorithms are groups of data-mining and nonparametric-based algorithms that use numerous independent variables in classification and regression applications.

Support vector machines (SVMs) are a family of classification and regression techniques that use statistical learning theory (Walton 2008). SVMs have emerged in recent times as a popular technique for data mining, with a great number of applications such as tissue classification (Furey et al. 2000; Pavlidis et al. 2004), shape extraction and classification (Cai et al. 2001; Du and Sun 2004), protein recognition (Zien et al. 2000), bakery process data (Rousu et al. 2003), hyperspectral data (Gualtieri and Cromp 1998), crop classification (Perales et al. 2003), and regression problems (Mukherjee et al. 1997; Pontil et al. 1998; Sivapragasam et al. 2001; Gao et al. 2003; Bray and Han 2004).

Support vector regression (SVR) is the application of SVM in regression, where the output is in real or continuous numbers (Mustakim et al. 2016). The aim of this study was to assess SPOT-HRG satellite data and SVM model regression as tools for estimating aboveground tree carbon stock in Darabkola forest in Mazandaran Province, Iran.

Materials and methods

Study area

The study area was located in the Hyrcanian Forests, District One of Darabkola's forests, in northern Iran (Fig. 1). Darabkola's forest, with an area of about 2612 ha, is a natural, nd mature forest with uneven-aged and dense to semidense stands. These comprise mixed hardwood types including *Fagus* dominant, mixed *Fagus*, *Carpinus–Fagus*, *Fagus–Carpinus*, and *Carpinus–Tilia*. Elevations range from 140 to 880 m, a.s.l., and the general slope in the study area is northerly, with subtle differences in slope aspects. Logging is performed by selecting individual trees in an attempt to approximate natural silviculture. The investigation was carried out in only one part of Darabkola's District One, about 1224 ha, where Persian beech (*Fagus orientalis*) is a dominant species (*Fagus* dominant type).

SPOT data (satellite for earth observation)

For this study, the images of the visible and near-infrared (VNIR) and short wave infrared or middle infrared (SWIR) subsystems were used from the SPOT HRG satellite data, acquired on 14 July 2009. The VNIR imagery contains three bands (green, red and near-infrared) with a spatial resolution of 10 m. The SWIR imagery has a spatial resolution of 20 m.

Field inventory data

We demarcated sampling plots on areas supporting relatively heterogeneous forest types. To reduce the effect of topography on illumination, we randomly selected plots with only a northern aspect. Plots were 30×30 m (0.36 ha) (Fig. 1) distributed in a cluster with north–south and east–west directions. The central position of each plot was accurately registered using a high quality handheld ground control point (STONEX SD7 model) device several times to get an accurate position. In each plot, for all trees with breast-height diameter greater than 7.5 cm, we recorded tree species, diameter at breast height (DBH). For some trees in each plot, we also measured height. The volume per hectare in each plot in natural forest was calculated based on tariff tables (Anonymous 2005) for the Darabkola Forest and using Eq. (1) for a forest plantation.

$$B_A = d^2 \frac{\pi}{4},\qquad(1)$$

where B_A is base area and d is diameter at breast height. To determine the amount of biomass, densities of all species

Fig. 1 Location of plots in Darabkola's forestry district, Mazandaran Province, northern Iran
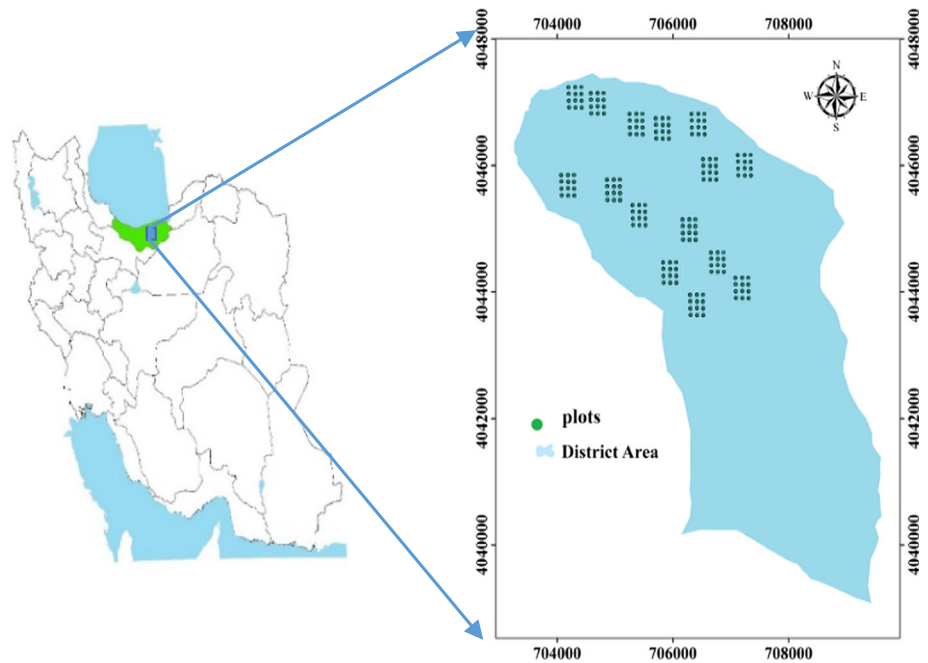
were measured in the laboratory, and then using Eq. (2) in closed forests with wet weather, the amount of biomass in the plot was calculated (FAO 1997).

$$B = V_{OB}W_DB_{EF}, \tag{2}$$

where, B is biomass, V_{OB} is the volume of trees, W_D is tree density by species, B_{EF} is a biomass expansion factor (FAO 1997). For calculating the amount of stored carbon, biomass values were multiplied by conversion coefficients, which are generally considered to be 50% (Eckert 2010; Goetz et al. 2009; Gibbs et al. 2007).

Image processing

The visible and near-infrared (VNIR) and short wave infrared or middle infrared (SWIR). Images were geometrically orthorectified using a 10-m resolution digital elevation model (DEM) and 37 control points obtained by a handheld GPS (3–5 m accuracy). The obtained root mean square errors (RMSEs) of imagery were less than 0.59 pixels for VNIR and 0.5 pixel for SWIR images. Geometric precision of the images was also verified using a road vector layer and unused collected GPS control points to rectify the accuracy of geometric rectification. Also, COST atmospheric correction method was used in this research. Studies have shown that the green and then red and near-infrared bands have the greatest darkness and that the amount of the SWIRv band is close to zero. With the atmospheric correction bands, atmospheric error rate was reduced.

Some commonly used vegetation indices (Table 1) for quantifying the vegetation attributes and enhancing the biophysical characteristics were generated using the VNIR

Table 1 Vegetation indices used of this study

Vegetation index	Formula	References
D_{VI}	$N_i - R$	Tucker (1979)
G_{DVI}	$N_i - G$	Tucker (1979)
N_{DVI}	$\frac{(N_i - R)}{(N_i + R)}$	Rouse et al. (1973)
N_{DWI}	$\frac{(R - SWIR)}{(R + SWIR)}$	Geo (1996)
N_{LI}	$\frac{(N_i^2 - R)}{(N_i^2 - R)}$	Goel and Qin (1994)
R_{DVI}	$\frac{(N_i - R)}{(\sqrt{N_i} + R)}$	Roujean and Breon (1995)

D_{VI} difference vegetation index, G_{DVI} green difference vegetation index, N_{DVI} normalized difference vegetation index, N_{DWI} normalized difference WASTER index, N_{LI} nonlinear index, R_{DVI} renormalized difference vegetation index, N_i near infrared, R red band, G green band, $SWIR$ shortwave infrared

and SWIR imagery. Principal component analysis (PCA) is normally performed in two standard ways: (1) using all bands and (2) selecting bands having the highest correlations. In this study, both methods were applied separately for VNIR and SWIR bands.

Characteristics for each of the bands of green, red, near infrared and SWIR using a gray level co-occurrence matrix (GLCM) were used to assess the texture of the image. GLCM is a tabulation of different constituents of pixel values in an image (Dutta et al. 2012). In this study, to assess the characteristics of texture matrix, occurrence and co-occurrence were used. In total, 30 independent variables and predictors were used in the analysis to predict the forest attributes.

Extraction of spectral values

In remote sensing, each pixel of the digital images has a numerical value that reflects the spectral behavior of the corresponding phenomena on the Earth's surface. In this study, postproduction of synthetic bands and measurement of the characteristics of the samples through field operation were performed, and the spectral values corresponding to plots of the original and synthetic bands were extracted. Then the obtained values and the corresponding spectral values of the corresponding pixels in the satellite data as well as the statistical relations were examined.

Modeling

In this study, an SVM was for modeling. An SVM is a nonlinear generalization of the generalized portrait algorithm developed by Vapnik (1995). Generally, SVMs focus on the boundary between classes and map the input space created by independent variables using a nonlinear transformation according to a kernel function. Linear, polynomial, radial basis function (RBF), and sigmoid are the four most commonly used kernel types. RBF is the most popular kernel used in SVMs (Cortez and Morsis 2007; Durbha et al. 2007). The simplicity of the method is one of its main advantages over other data mining techniques, such as artificial neural networks (ANNs). Thus, only a few parameters need to be adjusted by the users to optimize the model.

A prerequisite for SVM to achieve better results is to determine the parameters that play a key role in achieving high accuracy and provide better performance (Wang et al. 2009). The specified grid search using v-fold cross-validation (Durbha et al. 2007) is the most commonly used method to find appropriate values for the parameters, i.e., epsilon (ε) and capacity (C) with fixed a gamma that would produce high-accuracy results. A brief description of the proposed methods was summarized by Durbha et al. (2007). In this study, four different cores, including linear, polynomial, circular and radial basis function were used. Equation (3) was used to calculate the scale where n is equal to the number of variables (Hsu et al. 2010).

$$\gamma = 1/n,.\tag{3}$$

To choose the best ε and C values, we used the grid search method (Hsu et al. 2010), wherein C values ranged from 1 to 50, equal to the range of input variables (Mattera and Haykin 1999), and ε values from 0.1 to 0.5.

Model validation

The validity of the model was determined in a number of ways. Using 30% of samples, models were selected according to the significance of RMSE (in reverse order) and the t test

for bias (based on the t_Student). RMSE is the arithmetic mean of square errors, which was applied to the regression models to determine the accuracy of the estimate (Eq. 4).

$$R_m = \sqrt{\frac{\sum_{i=1}^n \left(\hat{C}_i - C_i \right)^2}{n}},\tag{4}$$

where R_m is the root mean square error, $\hat{C}_i$ is the carbon estimate based on the regression model for each plot of sample, C_i is the carbon measured in the control plots on the ground, and n is the number of control samples. After the model was obtained, the precision (P_r) of the calculation prediction needed to be examined using Eq. (5) (Li 2010; Dong et al. 2013).

$$P_r = \frac{\sum_{i=1}^n \left[1 - \text{abs}\left(\frac{\hat{C}_i - C_i}{C_i} \right) \times 100 \right]}{n}.\tag{5}$$

Bias (B_i, disambiguation) or systematic error is a way of estimating regression models used to determine authenticity. Biases for all models of the study were calculated using Eq. (6).

$$B_i = \frac{\sum_{i=1}^n \left(\hat{C}_i - C_i \right)}{n}.\tag{6}$$

Student's t test was used to assess the significance of the bias and the significance was analyzed by applying Eq. (7) (Ranta et al. 1991).

$$t = \frac{B_i}{S_D / \sqrt{n}},\tag{7}$$

where S_D is the standard deviation of the residuals ($\hat{C}_i - C_i$).

Results

Statistical analysis of field data and the extracted spectral bands

Of the 165 plots, 117 were used for modeling, while 48 were utilized for validation. Overall, 81 plots were in natural forest areas and 84 plots in afforestation. Average carbon storage was 206 tons per hectare, which was greater than the average carbon stored in afforestation (151 tons per hectare) and less than in natural forest at 264 tons of carbon per hectare. The maximum carbon stored in natural forests was 495.88 tons per ha, whereas the minimum of 55.8 tons per ha was estimated for afforested stands (Table 2).

The best value obtained for ε was equal to 0.1; however, the value of the parameter C fluctuated from 13 to 50. Excluding the linear model, the value of gamma remained

Table 2 Specifications and a descriptive assessment model for aboveground carbon stock

Parameters	Natural forest		Afforestation		Entire region	
	Validation	Training	Validation	Training	Validation	Training
Number	22	59	26	58	48	117
Average (t/ha)	235	264	149	151	189	206
Standard deviation	76	90	49	55	76	91
Maximum	375	495	254	254	375	495
Minimum	123	99	78	55	78	55

unchanged for all models according to the equation used in the calculation. The parameters for prediction and modeling kernels in each run were used to obtain the best results. The specified grid search for different models in the entire study area, including natural forest and afforestation area, are given in Table 3.

The results of SVR implementations determined by cross validation for carbon stock estimations are given in Table 4. The results of the carbon stock estimation for the entire region showed a lower relative RMSE and bias using a three-degree polynomial kernel type.

In carbon stock estimation using SVR in afforestation, the best results based on relative RMSE and bias were obtained using a polynomial kernel type. The validation results showed that the three-degree polynomial model in the afforestation with the remaining 67.05 t/ha root mean square error and estimation accuracy 64.3% is the best model for predicting carbon stocks in this area (Table 5).

Evaluation of the best model in the natural forest showed that the third degree polynomial had the lowest root mean square error (100.81 t/ha) among the four models, accuracy of the best forecast model for the forest area was 57.37, lower than the accuracy calculated for the best selected models in the entire area and the forest range (Table 5).

The correlation between the number of artificial bands, PCA, texture analysis and indexes are shown in Table 6. Results showed the most of the bands were negatively correlated.

Using the best model forecast map, the distribution of carbon in Table 6 in the region was prepared to show the spatial distribution of these variables in the region. This map can be used to identify areas with high carbon storage and apply the necessary measures. Areas marked in red have the lowest amount of carbon stored in the study area, and dark green colors represent areas with high carbon stocks in the entire area of the study (Fig. 2).

The average amount of carbon stored related to classes IV and V are located mostly within natural forest and also points to the low carbon often seen in the afforestation area.

Discussion

Forests play an important role in global change on Earth. Deforestation and forest degradation can result in carbon emission to the atmosphere, thus affecting global climate and environmental change (Hansen et al. 2015). Current concerns for global change and ecosystem functioning require accurate biomass estimation and examination of its dynamics (Zhou and Hemstrom 2009). Carbon sequestration potential in terms of plant species and in siting management practices, is different. Remote sensing data provides nondestructive and continuous detection information on the biomass of forest ecosystem.

In this study for estimating carbon stock using SPOT-HRG satellite data, correlations between carbon stock reflectance in SPOT-HRG spectral bands and forest

Table 3 SVM analysis results to determine the best parameters using the grid search for carbon stocks characteristic for the entire region, natural forests, and afforestation

Model	Entire region			Natural forests			Afforestation		
	Gamma	Capacity	Epsilon	Gamma	Capacity	Epsilon	Gamma	Capacity	Epsilon
	–	19	0.1	–	15	0.1	–	47	0.1
Linear	0.016	13	0.1	0.016	50	0.1	0.016	50	0.1
Polynomial (third degree)	0.016	27	0.1	0.016	50	0.1	0.016	50	0.1
R_{BF}	0.016	50	0.1	0.016	50	0.1	0.016	50	0.1

R_{BF} is radial basis function

Table 4 The results validate the various models in the entire region and afforestation area

Model	Entire region						Afforestation area					
	R_{MSE}	R_{MSE} (%)	Bias	Bias (%)	P (%)	t	R_{MSE}	R_{MSE} (%)	Bias	Bias (%)	P (%)	t
Linear	126.74	66.97	42	22.20	32.02	3.19	133.11	88.77	68.05	45.38	35.01	6.97
Polynomial (third degree)	72.69	38.41	10.04	5.31	62.2	0.91	67.05	44.71	3.47	2.31	64.3	0.36
R_{BF}	93.24	49.27	19.36	10.23	56.01	1.76	66.69	44.72	29.19	19.46	56.54	2.99
Sigmoid	102.41	54.11	23.03	12.17	48.48	2.09	73.23	48.84	29.71	19.81	53.36	3.04

R_{MSE} is root mean square error, Bias is disambiguation. R_{BF} is radial basis function

Table 5 The results validate the various models in the natural forest

Model	R_{MSE}	R_{MSE} (%)	Bias	Bias(%)	P (%)	t
Linear	151.47	64.27	76.71	32.55	36.68	4.69
Polynomial (degree 3)	100.81	42.77	39.09	16.58	57.37	2.39
R_{BF}	137.04	58.14	49.09	20.83	45.51	3.00
Sigmoid	112.47	47.72	43.47	18.44	55.01	2.66

R_{MSE} is root mean square error, B_{ias} is disambiguation, R_{BF} is radial basis function

Table 6 Correlation between artificial and carbon bands in the entire region

Bands	Correlation	Bands	Correlation
M	−0.442	N_{WVI}	−0.377
P_{CAa}	−0.423	M_{SI}	−0.371
PCA_b	−0.422	R_{atio}	−0.354
D_{VI}	−0.405	S_R	−0.354
N_{LI}	−0.393	M_{SR}	−0.351
R_{DVI}	−0.385	S_{VR}	−0.351
GDVI	−0.379	N_{DVI}	−0.347

P_{CA} principal component analysis, D_{VI} difference vegetation index, M Mean Near infrared, N_{LI} nonlinear index, R_{DVI} renormalized difference vegetation index, G_{DVI} green difference vegetation index, M_{SI} moisture stress index, R_{atio} ratio vegetation index, S_R simple ratio, M_{SR} modified simple ratio, N_{DVI} normalized difference vegetation index; S_{VR} shortwave infrared to visible ratio, N_{LI} Non-Linear Index, N_{WVI} normalized difference WASTER index

Fig. 2 Carbon distribution map of the study

attribute were low and negative. These negative correlation values for stand volume and biomass are in line with previous studies (Shataee et al. 2012). This negative value means that with increasing age of stands and number of canopy stories, the amount of shadow increases, leading to a reduction of the overall spectral response. An important point is the negative correlation between the bands and the indicators obtained from SPOT-HRG with the carbon indicator, implying that as carbon storage increases indicator values go down. This negative value in the natural forest means that with increasing age of stands and number of canopies, the amount of shadow increases, leading to a reduction in the overall spectral
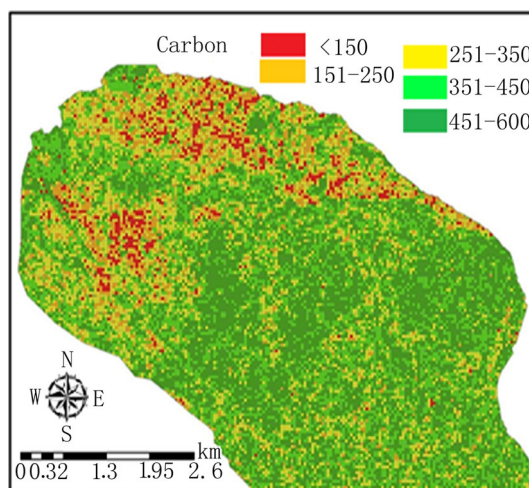
response. Thus, spectral reflection in the infrared section is lowered, and the increase in biomass leads to reduced spectral reflection. Naturally, the carbon that has accumulated over time reduces the reflection, allowing the indicator to appear in satellite images. A wide range of spectral indicators, along with reflection values of different bands, were considered. The results indicated that the red band and the RVI have the highest correlation with biomass, $R^2 = 0.48$ and $R^2 = 0.58$, respectively.

The results showed that the average carbon stored in natural forest is higher than in the afforestation, which has young trees (approximately 23 years) with low diameter,

thus lower volume and lower carbon stock than in older trees.

In this study derivatives of the NIR band and NIRs, including the NDVI index, are highly correlated with above ground carbon stock, similar to those of Gao et al. (2000), Todd et al. (1998) and Tucker (1979), who showed that the NDVI index is not useful for forest areas where vegetation is dense.

With respect to statistical applications, textural analyses are very useful since they provide much more information compared with spectral characteristics, especially for cases where large variations are caused in the information spectrum by a heterogeneous stand forest (Wulder et al. 1998). Texture measures are very sensitive to the spectral reflectance of forest canopy. Observations by Eckert (2012) confirmed that the more homogeneous a forest canopy structure is, the stronger the correlation between biomass and textural parameters; the issue is more relevant when high-resolution images are used (Tuominen and Pekkarinen 2005). Kajisa et al. (2009) used generalized linear model (GLM) to merge the data obtained from field statistics and remote sensing data to present a model for estimating biomass in the forest. Among other factors, this study also uses textural characteristics extracted from satellite images, which showed that the highest average was obtained for the infrared band, in line with the findings of Sohrabi et al. (2010), who compared various bands for estimating the stored volume in each segment and reported that the infrared band was best.

In previous studies, linear regression (Mitchard et al. 2009; Chen et al. 2009) and machine learning such as artificial neural network (ANNs) (Wijaya et al. 2010; Amini and Sumantyo 2009) were used to estimate aboveground biomass (AGB). The present study for modeling used support vector machine (SVM) regression. SVM is an important statistical learning algorithm to estimate forest parameters using remote sensing data (Shataee et al. 2012). Its advantage is its ability to use less training sample data to produce relatively higher accuracy for classification or estimation than other approaches.

On the basis of our results, the third-degree polynomial model was the best model for the entire study area, natural forest and afforestation with $R_{MSE} = 77.69$ t/ha, 100.81 t/ha and 67.05 t/ha, respectively, to estimate carbon stocks. The results of this study showed that SPOT-HRG satellite data can be useful in estimating carbon stocks.

References

Amini J, Sumantyo JT (2009) Employing a method on SAR and optical images for forest biomass estimation. IEEE Trans Geosci Remote Sens 47:4020–4026

Anonymous (2005) Darabkola Forest Management. Organization of Forest and Range and Watershed Management, Islamic Republic of Iran, pp 350

Bray M, Han D (2004) Identification of support vector machines for runoff modeling. Journal of Hydroinfor 6(4):265–280

Brown S (1997a) Estimating biomass and biomass change of tropical forests. FAO Forest Resources Assessment Publication, Roma, p 55

Brown S (1997b) Estimating biomass and biomass change of tropical forests: a Primer. (FAO Forestry Paper—134). Reprinted with corrections 1997.Produced by: Forestry Department. http://www.fao.org/docrep/w4095e/w4095e00.htm

Cai YD, Liu XJ, Xu X, Zhou GP (2001) Support vector machines for predicting protein structural class. Bioinformatics 2:3

Castillo-Santiago MA, Ricker M, De Jong BHJ (2010) Estimation of tropical forest structure from SPOT-5 satellite images. Int J Remote Sens 31:2767–2782

Chen WJ, Blain D, Li JH, Keohler K, Fraser R, Zhang Y (2009) Biomass measurements and relationships with Landsat-7/ETM + and JERS-1/SAR data over Canada's western sub-arctic and low arctic. Int J Remote Sens 30:2355–2376

Cortez P, Morsis A (2007) A data mining approach to predict forest fires using meteorological data. In: Neves J, Santos MF, Machado JM (eds.) Proceedings of the EPIA 2007—Portuguese conference on artificial intelligence, Guimarães, Portugal Heidelberg: Springer, pp 512–523

Dong J, Wang L, Xu S, Zhao R (2013) Comparison of four models on forest above ground biomass estimation based on remote sensing. Geo Infor Resour Manag Sustain Ecosyst 398:253–263

Du CJ, Sun DW (2004) Shape extraction and classification of pizza base using computer vision. J Food Eng 64:489–496

Durbha SS, King RL, Younan NH (2007) Support vector machines regression for retrieval of leaf area index from multiangle imaging spectroradiometer. Remote Sens Environ 107:348–361

Dutta S, Datta A, Das Chakladar N, Pal SL, Mukhopadhyay S, Sen S (2012) Detection of tool condition from the turned surface images using accurate grey level co-occurrence technique. Precis Eng 36:458–466

Eckert S (2012) Improved forest biomass and carbon estimations using texture measures from worldview-2 satellite data. Remote Sens 4:810–829

Eckert S, Rakoto Ratsomba H, Rakotondrasoa LO, Rajoelison LG, Ehrensperger A (2010) Deforestation and forest degradation monitoring and assessment of biomass and carbon stock of lowland rainforest in the Analjirofo region, Madagascar. For Ecol Manag 262:1996–2007

FAO (1997) Estimating biomass and biomass change of tropical forests: a primer. FAO Forestry Paaper, p 134

Furey TS, Cristianini N, Duffy N, Bednarski DW, Schummer M, Haussler D (2000) Support vector machine classification and validation of cancer tissue samples using microarray expression data. Bioinformatics 16(10):906–914

Gao X, Huete AR, Ni W, Miura T (2000) Optical-biophysical relationships of vegetation spectra without background contamination. Remote Sens Environ 74:609–620

Gao JB, Gunn SR, Harris CJ (2003) SVM regression through variational methods and its sequential implementation. Neurocomputing 55:151–167

Geo BG (1996) NDWI-A normalized difference water index for remote sensing of vegetation liquid water from space. Remote Sens Environ 58:257–266

Gibbs HK, Brown S, Niles JO, Foley JA (2007) Monitoring and estimating tropical forest carbon stocks: making REDD a reality. Environ Res Lett 2(4):1–13

Goel NS, Qin W (1994) Influences of canopy architecture on relationships between various vegetation indices LAI and FPAR: a computer simulation. Remote Sens 10:309–347

Goetz SJ, Baccini A, Laporte NT, Johns T, Walker W, Kellndorfer J (2009) Mapping and monitoring carbon stocks with satellite observations: a comparison of methods. Carbon Balance Manag 4(2):1–7

Gualtieri JA, Cromp RF (1998) Support vector machines for hyperspectral remote sensing classification. Proc SPIE 3584:221–232

Hansen EH, Gobakken T, Solberg S, Kangas A, Ene L, Mauya E, Næsset E (2015) Relative efficiency of ALS and InSAR for biomass estimation in a Tanzanian rainforest. Remote Sens 7:9865–9885

Hsu CW, Chang CC, Lin CJ (2010) A practical guide to support vector classification (Taipei: Department of Computer Science, National Taiwan University). http://www.csie.ntu.edu.tw/~cjlin

IPCC (2000) Nakićenović N, Swart R (eds) Special report on emissions scenarios: a special report of Working Group III of the intergovernmental panel on climate change (book), Cambridge University Press

Intergovernmental Panel on Climate Change (IPCC) (2007) The physical science basis: working group I contribution to the fourth assessment report of the IPCC. Cambridge University Press, Cambridge, p 996

Kajisa T, Murakami T, Mizoue N, Top N, Shigejiro Y (2009) Object-based forest biomass estimation using Landsat ETM + in Kampong Thom Province, Cambodia. For Res 14:203–211

Li M (2010) Estimation and analysis of forest biomass in northest forest region using remote sensing technology. Estimation of canopy-average surface-specific leaf area using Landsat TM data. Northoest Forestry University, Harbin

Liu Q, Yang L, Liu Q, Li J (2015) Review of forest above ground biomass inversion methods based on remote sensing technology. J Remote Sens 19:62–74

Mattera D, Haykin S (1999) Support vector machines for dynamic reconstruction of a chaotic system. In: Schölkopf B, Burges J, Smola A (eds) Advances in kernel methods: support vector machine. Cambridge, MA, MIT Press, pp 211–241

Mitchard ETA, Asstchi SS, Woodhouse IH, Nangendo G, Ribeiro NS, Williams M (2009) Using satellite radar backscatter to predict above-ground woody biomass: a consistent relationship across four different African landscapes. Geophys Res Lett 36:1–6

Mukherjee S, Osuna E, Girosi. F (1997) Nonlinear prediction of chaotic time series using support vector machines. In Proceeding of the 1997 IEEE workshop, pp 511–520

Mustakim M, Buono A, Hermadi I (2016) Performance comparison nSSION and artificial neural network for prediction of oil palm production. J Comput Sci Inf 9(1):1–8

Pavlidis P, Wapinski I, Noble WS (2004) Support vector machine classification on the web. Bioinformatics 20(4):586–587

Perales FJ, Campilho AJC, Blanca NP, Sanfeliu A (eds) (2003) Pattern recognition and image analysis. In: Lecture notes in computer science, Berlin, Germany Springer-verlag Berlin Heidelberg, pp 134–141

Pontil M, Mukherjee S, Girosi F (1998) On the noise model of support vector machine regression. In Proceedings of the 11th international conference on algorithmic learning theory, Institute of Technology Cambridge, Massachusetts, USA pp 316–324

Ranta E, Rita H, Kouki J (1991) Biometria. Yliopistopaino, Tilastotiedettä ekologeille. Helsinki, p 569

Roujean JL, Breon FM (1995) Estimating PAR absorbed by vegetation from bidirectional reflectance measurement. Remote Sens Environ 51:375–384

Rouse JW, Haas RH, Schell JA, Deering DW (1973) Monitoring vegetation systems in the Great Plains with ERTS. In: Third earth resources technology satellite-1 symposium. Washington: published by NASA, vol 1, pp 309–317

Rousu J, Flander L, Suutarinen M, Autio K, Kontkanen P, Rantanen A (2003) Novel computational tools in bakery process data analysis: a comparative study. J Food Eng 57(1):45–56

Shataee Sh, kalbi S, Fallah A (2012) Forest attribute imputation using machine-learning methods and ASTER data: comparison of k-NN, SVR and random forest. Regression algorithms. Int J Remote Sens 33(19):6254–6280

Sironen S, Kangas A, Maltamo M (2010) Comparison of different non-parametric growth imputation methods in the presence of dependent observations. Forestry 83:39–51

Sivapragasam C, Liong SY, Pasha MFK (2001) Rainfall and runoff forecasting with SSA–SVM approach. Journal of Hydroinf 3:141–152

Sohrabi H, Hosseini SM, Zobeiri M (2010) Assessment the forest volume stocks by the use of aerial texture indexes. Iran J For Poplar Res 18(2):297–306

Steininger MK (2000) Satellite estimation of tropical secondary forest above-ground biomass: data from Brazil and Bolivia. Int J Remote Sens 21:1139–1157

Todd SW, Hoffer RM, Milchunas DG (1998) Biomass estimation on grazed and ungrazed rangelands using spectral indices. Int J Remote Sens 19:427–438

Tucker CJ (1979) Red and photographic infrared linear combinations for monitoring vegetation. Remote Sens Environ 8:127–150

Tuominen S, Pekkarinen A (2005) Performance of different spectral and textural aerial photograph features in multi-source forest inventory. Remote Sens Environ 94:256–268

Vapnik V (1995) The nature of statistical learning theory. Springer, New York, p 768

Vicharnakorn P, Shrestha RP, Nagai M, Salam AP, Kiratiprayoon S (2014) Carbon stock assessment using remote sensing and forest inventory data in Savannakhet, Lao PDR. Remote Sens 6:5452–5479

Walton JT (2008) Subpixel urban land cover estimation: comparing cubist, random forests, and support vector regression. Photogramm Eng Remote Sens 74(10):1213–1222

Wang Y, Wang J, Du W, Wang C, Liang Y, Zhou C, Huang L (2009) Immune particle swarm optimization for support vector regression on forest fire prediction. In: Yu W He H, Zhang N(eds) Advances in neural networks, ISNN 2009, Part II, LNCS 5552, Berlin: Springer, pp 382–390

Wijaya A, Liesenberg V, Gloaguen R (2010) Retrieval of forest attributes in complex successional forest of Central Indonesia: modeling and estimation of bitemporal data. For Ecol Manag 259:2315–2326

Wulder MA, LeDrew EF, Franklin SE, Lavigne MB (1998) Aerial image texture information in the estimation of northern deciduous and mixed wood forest leaf area index (LAI). Remote Sens Environ 64:64–76

Zhou X, Hemstrom MA (2009) Estimating aboveground tree biomass on forest land in the Pacific Northwest: a comparison of approaches. Publication series: Research Paper, Department of Agriculture, Forest Service, Pacific Northwest Research Station, p18

Zien A, Rätsch G, Mika S, Schölkopf B, Lengauer T, Müller KR (2000) Engineering support vector machine kernels that recognize translation initiation sites. Bioinformatics 16(9):799–807